

collision-free lifetimes of the interacting levels were not experimentally available because the fluorescence intensities from these levels were low.

In the case of the NO molecule, an intense interaction between $B^2\Pi(v=1)$ and $b^4\Sigma^-(v=0)$ has been reported,²¹ and it appears as another candidate for single rovibronic LIF study of doublet–quartet interaction. It is hardly possible, however, to excite the perturbed vibronic level NO $B^2\Pi(v=1)$ because of the extremely small Franck–Condon factor between $B^2\Pi(v=1)$ and $X^2\Pi(v=0)$.

(iii) *Collisional Influence on Intersystem Crossing.* The collisional influence on intersystem crossing is another important aspect to be discussed. The buildup time that appeared in the fluorescence for excitation to the strongly perturbed rovibronic level (see section 3(iii)) is well ascribed to the collision-induced excitation transfer: The selective excitation to a perturbed level is followed by a collisional redistribution of energy to the rovibronic levels of pure $B^2\Pi$ character which have shorter radiative lifetimes than the perturbed level initially prepared. The reciprocal plots shown in Figure 9 of τ_{rise} would reduce to zero at zero pressure. The rates of collisional excitation transfer are only tentative values because they are derived from the linear dependence in a limited range of N_2 pressure. The simple two-level model mentioned above should be refined with the consideration of collision-induced rotational randomization.

The collisional transfer is also responsible for the slow decay component which reveals itself toward a higher pressure in the fluorescence from the $v' = 11$ state (see section 3(ii)): The selective excitation to any rotational level of the $v' = 11$ state is followed by a rotational redistribution to many nearby levels, among which is the specific perturbed level. The collision-induced excitation

transfer takes place to the $b^4\Sigma^-(v'=10)$ state through the specific “gate” level. Then the return to $B^2\Pi$ is buffered by $b^4\Sigma^-$, and the slow component is brought about in the fluorescence decay.

In spite of the existence of intersystem crossing with $b^4\Sigma^-$ at high J rotational levels ($J' = 36.5$ and 42.5 of the f and e components, respectively), the measured rotational levels of $B^2\Pi_{1/2^-}(v'=9)$ reveal single exponential fluorescence decay even at high pressures in comparison with those of $v' = 11$. This is because the rotational redistribution to such high- J gate levels is insignificant from thermal considerations, and the collision-induced intersystem coupling scarcely takes place.

5. Concluding Remark

A time domain LIF observation of NS $B^2\Pi$ interacted by $b^4\Sigma^-$ and $B^2\Sigma^+$ has been carried out by the use of a pulsed excitation to a single rovibronic level studied spectroscopically by Jenouvrier and Pascat.⁴ The influences of doublet–quartet interactions on the fluorescence from the NS $B^2\Pi$ state are summarized as follows: (a) The radiative lifetimes of rovibronic $B^2\Pi$ states of mixed character with $b^4\Sigma^-$ are longer than those of pure $B^2\Pi$ rovibronic states. (b) The buildup time and long decay component are brought about by collision-induced intersystem interaction. (c) In the high-pressure limit, any rotational level, either perturbed or not, exhibits a multiexponential decay profile. The slow component involved therein is the consequence of the collision-induced excitation transfer between the interacting electronic states.

The pure NS $B^2\Pi(6 \leq v' \leq 12)$ states are found to have a little shorter radiative lifetime, 1.01–1.29 μs , than the NO $B^2\Pi$ vibronic states. An exceptionally fast fluorescence quenching rate is obtained for the $B^2\Pi(v'=12)$ state, being ascribed to the influence of collision-induced predissociation.

Registry No. NS, 27954-72-9.

(21) E. Miescher, *J. Chem. Phys.*, **73**, 3088 (1980).

Formation of Ozone in the Reaction of OH with O_3^- and the Decay of the Ozonide Ion Radical at pH 10–13

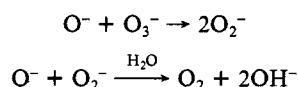
K. Sehested,* J. Holcman, E. Bjergbakke, and Edwin J. Hart†

Accelerator Department, Risø National Laboratory, DK 4000 Roskilde, Denmark (Received: March 21, 1983; In Final Form: June 7, 1983)

Ozone forms in aqueous alkaline solutions, pH 10–13, by a reaction between OH and O_3^- radicals. The reaction, $OH + O_3^- \rightarrow O_3 + OH^-$, is about 30% of the total reaction. A second reaction is $OH + O_3^- + OH^- \rightarrow 2O_2^- + H_2O$. The ozone formation is demonstrated by a high-pressure pulse radiolysis technique using a 4- μs , 40-krd pulse. The ozone rapidly disappears in a reaction with the simultaneously formed O_2^- re-forming O_3^- . The product resulting from the O_3^- decay is the peroxy radical, O_2^- . The overall rate constant, $k(OH + O_3^-)$, is $(8.5 \pm 1.0) \times 10^9 \text{ dm}^3 \text{ mol}^{-1} \text{ s}^{-1}$. Computer simulations of the high-pressure system as well as of the atmospheric-pressure oxygenated system with high and low pulse intensity support a mechanism for the O_3^- decay based on the above-mentioned reactions. The protonation rate constant of the O_3^- radical ion, $k(O_3^- + H^+)$, is $(9.0 \pm 1.0) \times 10^{10} \text{ dm}^3 \text{ mol}^{-1} \text{ s}^{-1}$.

Introduction

In a previous paper¹ we reported on the ultraviolet spectrum and the decay of the ozonide ion radical, O_3^- , in strong alkaline solution at pHs in the range 13.0–13.8. A complete mechanism for the decay of O_3^- and formation of O_2^- at these high pHs was based on the following two reactions:



At these pHs, OH radicals are largely dissociated into O^- radicals

and consequently the OH radical reactions are unimportant in these experiments. However, O_3^- radicals also form at lower pHs (10–13), where OH radical reactions cannot be neglected since they are even more important than the O^- reactions. A study of the decay of O_3^- at these lower pHs has been undertaken.

Evidence of ozone formation by the reaction of OH radicals with the ozonide ion radical is reported and a mechanism for O_3^- disappearance is suggested. Ozone formation in a reaction of ozonide ion radicals and carbonate radicals has previously been published.²

* Present address: 2115 Hart Road, Port Angeles, WA 98362.

(1) Sehested, K.; Holcman, J.; Bjergbakke, E.; Hart, E. J. *J. Phys. Chem.* **1982**, *86*, 2066.

Experimental Section

Pulse Radiolysis. The 10-MeV HRC linear accelerator at Risø with pulse length of 1–4 μs and a dose measured in the pressure cell of 10–40 krd pulse⁻¹ was used throughout the work. The optical detection system, data storage, and treatment of data are described elsewhere.^{1,3} The computer simulations were performed on a Burroughs 7800 with a program developed for homogeneous kinetics on the basis of the algorithm DIFSUB by Gear.⁴

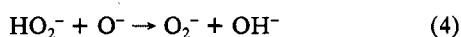
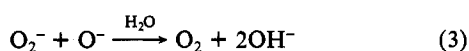
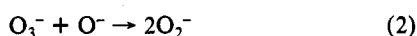
The construction, operation, and performance of the high-temperature pressure cell used in this investigation are described in previous papers.^{1,3} In the present study, the solutions were equilibrated at high pressures of N_2O and O_2 at room temperature, $\sim 20^\circ\text{C}$. Only the first pulse was used for the kinetic measurements, but even for these determinations several pulses do not alter the results to any significant degree.

Solutions. All solutions were prepared from triply distilled water. The water was saturated by air or oxygen at neutral pH, and the sodium hydroxide (Merck p.a.) was added just before closing the syringe in order to minimize the content of carbonate. N_2O and O_2 were used without further purification. In solutions where N_2O is present, 40 atm (4 MPa) of N_2O was always applied, providing a concentration of about 0.9 mol dm⁻³. The dosimetry was performed with a modified hexacyanoferrate(II) dosimeter⁵ using 10⁻² mol dm⁻³ $\text{Fe}(\text{CN})_6^{4-}$ and $\epsilon_{420} = 1000 \text{ dm}^3 \text{ mol}^{-1} \text{ cm}^{-1}$.

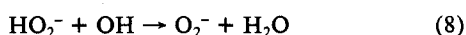
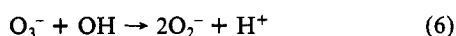
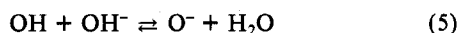
Results and Discussion

The spectrum of the ozonide ion radical, O_3^- , at pH 10–13 is identical with that at pH 13–13.8 published in our previous paper.¹ The absorbance of O_3^- at 430 nm is accounted for by a kinetic analysis of the data using standard G values for radical species (see later) and an extinction coefficient, $\epsilon(\text{O}_3^-)_{430}$, of 2000 dm³ mol⁻¹ cm⁻¹.

The product from the decay of O_3^- at pHs 10–13 is also the peroxy radical, O_2^- , although the yields are below these found at pHs above 13. We identified O_2^- by its spectrum and lifetime as at high pH¹ using our pressure cell technique. We also modified the mechanism for the decay of O_3^- at these lower pHs by taking into account the dissociation reactions of OH and H_2O_2 . The essential reactions which account for the decay of O_3^- and the formation of O_2^- at pH 13–13.8 are



These reactions and the following ones for the OH radicals were introduced in the reaction scheme for the computer calculations at lower pHs.



Except for the rate constant of reaction 6, all other rate constants in the 44 reactions in the computation program are well established.⁶ However, it is not possible with the above reaction scheme

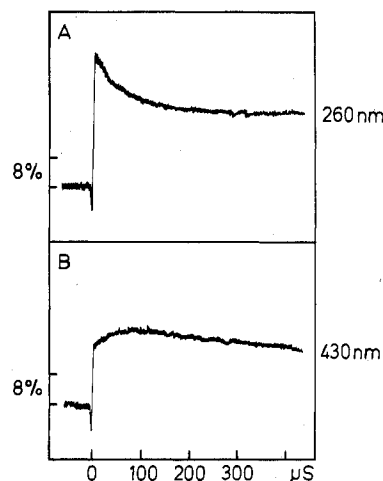
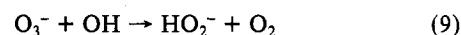
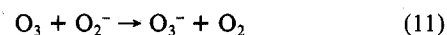


Figure 1. Oscilloscope traces of percent transmission vs. time at 260 and 430 nm obtained in pulse-irradiated 3×10^{-4} mol dm⁻³ sodium hydroxide solutions, pH 10.45, containing 1.25×10^{-3} mol dm⁻³ oxygen and ~ 0.9 mol dm⁻³ nitrous oxide; dose, 40 krd; pulse length, 4 μs ; optical path length, 2.5 cm.

to account for both the decay of O_3^- at 430 nm and the buildup of O_2^- at 240 nm. By simulation of the decay of O_3^- , the calculated yields of O_2^- are too high compared with experimental values. Therefore, we introduced two additional reactions of OH and O_3^- , namely



We exclude the reactions $\text{O}_3^- + \text{O}_3^-$ and $\text{O}_3^- + \text{O}_2^-$ since we find no second-order decay of O_3^- . The O_3^- lifetime is almost proportional to the oxygen pressure up to 10 MPa. None of the single reactions (reaction 6, 9, or 10) is able to explain the decay of O_3^- and the buildup of O_2^- . Reaction 6 yields too much O_2^- , reaction 9 followed by reaction 8 gives too little, and reaction 10 does not produce peroxy radicals. It is therefore likely that the reaction of OH radicals with O_3^- yields more than one product. Reaction 6, however, must take place since O_2^- is found as a product. Computer simulations based on reactions 6 and 9 do not fit the buildup kinetics of the UV absorbance. However, reactions 6 and 10 account for the final absorption of O_2^- , the buildup kinetics of O_2^- in the UV, and the decay kinetics of O_3^- at 430 nm. As a consequence of obtaining a good quality fit with reactions 6 and 10, reaction 9, even if it occurs, is unimportant. The ozone formed in reaction 10 has a stronger absorption than O_2^- at wavelengths above 220 nm,⁷ but it is rapidly consumed by the surplus of O_2^- re-forming O_3^- by the reaction⁸



$$k = 1.5 \times 10^9 \text{ dm}^3 \text{ mol}^{-1} \text{ s}^{-1}$$

Therefore, ozone cannot be seen as a final product, but has only a transient influence on the buildup kinetics and absorption in the UV, which makes it difficult to detect under usual conditions. The reactions of ozone with HO_2^- and OH^- do not influence the disappearance of ozone under our conditions, as these reactions are slow^{9,10} compared with reaction 11.

According to reaction 10, O_3 forms by the reaction of the OH and O_3^- radicals. This reaction was experimentally verified by using our high-pressure-cell technique with 4 MPa of N_2O and various oxygen concentrations at different pHs. Furthermore, we used a 4- μs pulse, delivering a dose in the pressure cell of 40

(2) Holcman, J.; Sehested, K.; Bjergbakke, E.; Hart, E. J. *J. Phys. Chem.* **1982**, *86*, 2069.

(3) Christensen, H.; Sehested, K. *Radiat. Phys. Chem.* **1979**, *16*, 183.

(4) Gear, C. W. *Commun. ACM* **1971**, *14*, 185–90.

(5) Rabani, J.; Matheson, M. S. *J. Phys. Chem.* **1966**, *70*, 761.

(6) Ross, A. B.; Neta, P. *Natl. Stand. Ref. Data Ser. (U.S., Natl. Bur. Stand.)* **1979**, *65*. Anbar, M.; Bambenek, M.; Ross, A. B. *Ibid.* **1973**, *43*. Farhatziz; Ross, Alberta B. *Ibid.* **1977**, *59*.

(7) Hart, E. J.; Sehested, K.; Holcman, J. *Anal. Chem.* **1983**, *55*, 46.

(8) Sehested, K.; Holcman, J.; Hart, E. J. *J. Phys. Chem.* **1983**, *87*, 1951.

(9) Forni, L.; Bahnemann, D.; Hart, E. J. *J. Phys. Chem.* **1982**, *86*, 255.

(10) Staehelin, J.; Hoigne, J. *Environ. Sci. Technol.* **1982**, *16*, 676.

TABLE I: Calculated and Measured Yields of Ozone at Various Pulse Lengths, Doses, and Oxygen Concentrations in Solutions Saturated at 4 MPa of N₂O

pulse length, μs	dose, krd	$10^3[\text{oxygen}],$ mol dm^{-3}	$10^6[\text{ozone}], \text{mol dm}^{-3}$			
			pH 12		pH 11	
			calcd	measd	calcd	measd
4	40	0.24	4.90	5.0 ± 0.5	2.8	3.0 ± 0.5
1	10	1.25	0.76	1.0 ± 0.7		
2	20	1.25	2.5	2.5 ± 0.5		
3	30	1.25	4.75	5.0 ± 0.7		
4	40	1.25	7.2	7.5 ± 0.7	8.5	9.0 ± 1.0
4	40	2.5	5.5	5.0 ± 1.0	10.4	10.0 ± 1.0
4	40	4.0	3.8	4.0 ± 1.5		
4	40	5.0	3.3		10.8	10.5 ± 1.0
1	10	6.25			1.4	1.0 ± 0.5
2	20	6.25			4.2	5.0 ± 1.0
3	30	6.25			7.6	7.5 ± 1.0
4	40	6.25	2.9		10.7	10.5 ± 1.0
4	40	10.0			9.8	9.5 ± 1.0
4	40	12.5			9.3	9.5 ± 1.0

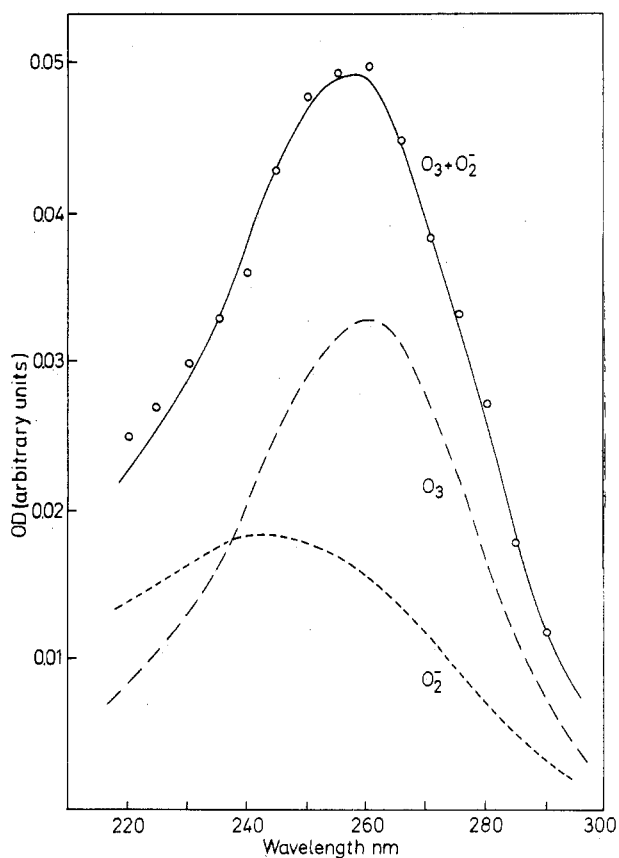


Figure 2. Optical spectrum of the decaying absorbance in the UV. Experimental results are normalized to the spectrum of equal amounts of O₃ and O₂⁻ at 245 nm. The solution was $5 \times 10^{-4} \text{ mol dm}^{-3}$ sodium hydroxide, pH 10.7; $1.25 \times 10^{-3} \text{ mol dm}^{-3}$ oxygen; $\sim 0.9 \text{ mol dm}^{-3}$ N₂O; pulse length, 4 μs ; dose, 40 krd; optical path length, 2.5 cm.

krd, to enhance O₃ formation by the reaction between OH and O₃⁻ radicals during the pulse.

The result, pictured in Figure 1A, shows an absorption at 260 nm just after the pulse, partly decaying in 150 μs . This transient absorption is on the background of the long-lived O₂⁻ absorption. Figure 1B shows a simultaneous buildup at the 430-nm band, as part of the 260-nm absorption decays. This absorption band at 430 nm has a spectrum similar to O₃⁻, thereby identifying the species as the ozonide ion radical. The spectrum of the decaying transient absorption at 260 nm, however, is not a spectrum of a known species (Figure 2), but it appears to be a composite of the absorptions of O₂⁻ and O₃. Indeed, if the spectra of equal amounts of these two species are added and normalized (Figure 2), the resulting spectrum matches the one taken just after the pulse (see

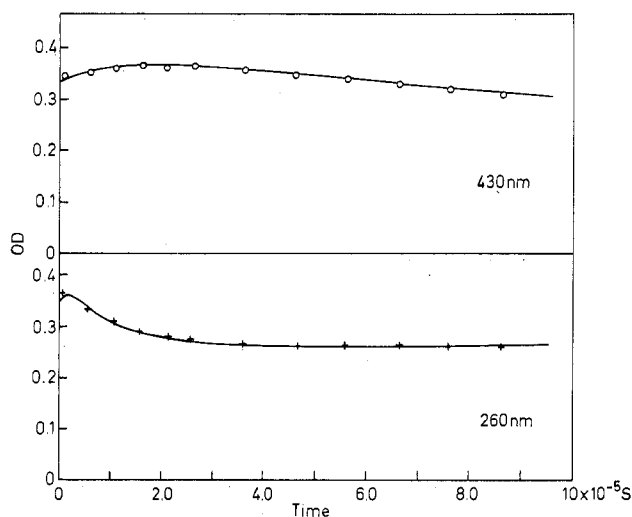


Figure 3. Calculated and measured OD for a 4- μs , 45-krd pulse at 260 and 430 nm. The solution was $1.15 \times 10^{-3} \text{ mol dm}^{-3}$ sodium hydroxide, pH 11.1; $1.25 \times 10^{-3} \text{ mol dm}^{-3}$ oxygen; $\sim 0.9 \text{ mol dm}^{-3}$ nitrous oxide; optical path length, 2.5 cm. Solid lines: calculated. O, +: experimental values.

curve designated O₃ + O₂⁻ of Figure 2).

The fact that equal amounts of O₂⁻ and O₃ account for the measured absorption, together with the additional formation of O₃⁻, indicates that reactions 10 and 11 take place. Computer calculations on the absorptions at 260 and 430 nm show a stoichiometric relation between O₃ and O₃⁻ as expected from reaction 11. Furthermore, the calculations require a rate constant, $k_{11} = 1.5 \times 10^9 \text{ dm}^3 \text{ mol}^{-1} \text{ s}^{-1}$, which coincides with the one earlier determined in ozone solutions.⁸

During a 4- μs pulse of 40 krd most of the radicals react in second-order radical-radical reactions. With a high concentration of N₂O ($\sim 0.9 \text{ mol dm}^{-3}$) and moderate pressure of oxygen, practically all hydrated electrons are converted into OH radicals, which react with each other forming hydrogen peroxide and through O⁻ with oxygen yielding O₃⁻. As these products build up, the OH radicals also react with them as well as with the secondary radicals. By adjustment of the pH and the oxygen concentration in a way which makes OH partly convert into O⁻ through reaction 5 and into O₃⁻ by the reverse of reaction 1, favorable conditions for studying the radical-radical reactions (eq 6 and 10) are created, especially at the end of a long pulse.

From the decay of the ozonide ion radical and from the formation of ozone and the final yields of the peroxy radical, the rate constants for reactions 6 and 10 are calculated. The values, which are consistent with all the results both at high and low doses and with and without N₂O at pH 10-13 (see below), are $k_6 = (6.0 \pm 0.7) \times 10^9 \text{ dm}^3 \text{ mol}^{-1} \text{ s}^{-1}$, and $k_{10} = (2.5 \pm 0.5) \times 10^9 \text{ dm}^3 \text{ mol}^{-1}$

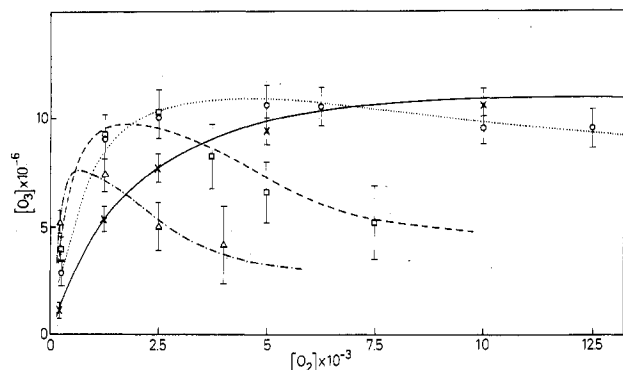


Figure 4. Calculated and measured yields of ozone as a function of pH and oxygen concentration in a solution saturated at 4 MPa of N_2O ; pulse, 4 μs ; dose, 40 krd; (— \times —) pH 10.5, (··· \circ ···) pH 11.0, (--- \square ---) pH 11.5, (-·- Δ -·-) pH 12.0.

s^{-1} . The overall rate constant for the OH radical reaction with the ozonide ion radical is then $k = (8.5 \pm 1.0) \times 10^9 \text{ dm}^3 \text{ mol}^{-1} \text{ s}^{-1}$. An example of a computer calculation including experimental values at a 45-krd pulse is shown in Figure 3.

Calculated yields of ozone based on the proposed mechanism with the above rate constants for k_6 and k_{10} together with experimental results under various conditions are shown in Table I and Figure 4. The experimental results are derived from the additionally formed O_3^- by extrapolation to the pulse end. As pH and oxygen concentration are increased, the background of O_3^- rises and the accuracy of the ozone determination becomes lower. The most favorable conditions for a high ozone yield are obtained in a 4- μs pulse, pH 11, with 4 MPa of N_2O and 0.3 MPa of O_2 and at pH 10.5 with 4 MPa of N_2O and 1.0 MPa of O_2 . O_3 formation is greatly enhanced by the pulse width and dose. At pH 12.5 and higher, the formation of O_3^- in reaction -1 is too fast even at low concentrations of oxygen to ensure enough OH radicals to participate in reactions 6 and 10. At pHs around 12 the OH radicals are also consumed to a great extent by the fast reaction, $OH + O^- \rightarrow HO_2^-$ ($2 \times 10^{10} \text{ dm}^3 \text{ mol}^{-1} \text{ s}^{-1}$) (see later). Figure 4 shows calculated and experimental yields of the ozone at various pHs as a function of the oxygen concentration for a 4- μs , 40-krd pulse.

From these results we conclude that reaction 10 is the source of the ozone with O_3^- and OH as the precursors. However, an electron-transfer reaction between OH and O^- has previously been suggested to be a potential source of ozone too.¹¹ This reaction was suggested to explain additional formation of $O^3(P)$ in alkaline solutions.¹² While the main product from this reaction is hydrogen peroxide, a small fraction may be an electron transfer from O^- to OH forming $O^3(P)$. The triplet oxygen atom so formed would under our conditions react rapidly with oxygen, forming ozone. We studied this possibility in a separate experiment at pHs 11 and 12. In a solution of pH 11 with 0.9 mol dm^{-3} N_2O and 6.25×10^{-3} mol dm^{-3} oxygen and a solution of pH 12 containing 0.9 mol dm^{-3} N_2O and 1.25×10^{-3} mol dm^{-3} oxygen, we calculate that 3.5 and 50.1 μM hydrogen peroxide, respectively, form in the reaction between OH and O^- in a 40-krd pulse at these two pHs. If any appreciable amount of ozone should arise from this reaction, it should be seen at pH 12 and not at pH 11. The calculated and measured yields of ozone at pH 11 are 10.7 and 10.2 μM , and at pH 12 are 4.9 and 5.0 μM , respectively. From these results we conclude that under our conditions the reaction between O_3^- and OH is the main source of ozone and that less than a few percent of OH reacting with O^- may produce oxygen atoms, a potential precursor of ozone.

Our system also enables us to determine the protonation rate of the ozonide ion radical. In experiments with ozone solutions⁸ it was demonstrated that O_3^- is formed in reactions of ozone with

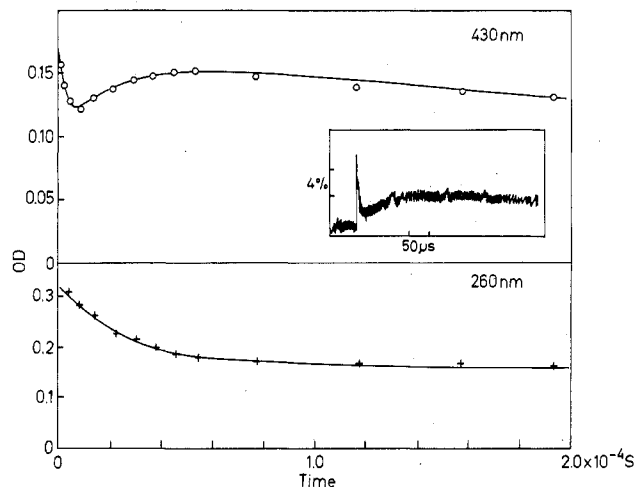


Figure 5. Calculated and measured OD for a 4- μs , 45-krd pulse at 260 and 430 nm. The solution was 1.1×10^{-4} mol dm^{-3} sodium hydroxide, pH ~ 10 ; 5×10^{-2} mol dm^{-3} oxygen; ~ 0.9 mol dm^{-3} nitrous oxide; optical path length, 2.5 cm. Solid lines: calculated O_3^- ; +: experimental values. Insert: Oscilloscope trace at 430 nm for a 4- μs , 40-krd pulse in a solution of 3×10^{-5} mol dm^{-3} sodium hydroxide (pH ~ 9.5), 0.1 mol dm^{-3} oxygen, ~ 0.9 mol dm^{-3} N_2O .

TABLE II: G Values for Primary Radicals, Molecular Products, and Ions Used in the Computations^a

	pH 13		pH 12-10	
	4 MPa of N_2O + 0.1 MPa of O_2	0.1 MPa of O_2	4 MPa of N_2O + 0.1 MPa of O_2	0.1 MPa of O_2
e_{aq}^-	3.7	2.8	3.7	2.8
H	0.55	0.55	0.55	0.55
OH	3.4	3.0	3.2	2.8
HO_2^- (H_2O_2)	0.6	0.6	0.7	0.7
H_2	0.205	0.455	0.205	0.455
O_2^-	0.02	0.02	0.02	0.02
H^+	4.22	3.32	4.22	3.32
OH^-	0.5	0.5	0.5	0.5

^a For explanation see ref 1.

hydrated electrons and peroxy radicals at pHs from 6 to 11. It was also found¹³ that the decay of O_3^- in the pH range 7-10 could be explained by the dissociation of O_3^- (reaction 1). And as discussed below, the faster decay in acid solution is due to protonation of O_3^- . Figure 5 shows the transient absorptions at 430 and 260 nm after irradiating a solution of 0.9 mol dm^{-3} N_2O and 5×10^{-2} mol dm^{-3} oxygen at pH 10 with a 40-krd pulse. See the insert taken at pH 9.5. The very fast decay of absorbance in the first few microseconds after the pulse is ascribed to the protonation of O_3^- . The transient pH change due to the pulse is so large at this pH that the solution is initially acid. The production of H^+ and OH^- in a 40-krd pulse is approximately 150 and 20 μM , respectively. As the initial concentration of OH^- in the solution is $\sim 10^{-4}$ mol dm^{-3} , the surplus of H^+ will produce a transient decrease in pH below 5 even with the fast neutralization reaction between H^+ and OH^- . It is, however, possible to form small amounts of O_3^- from the competition between water ($k = 2 \times 10^6 \text{ dm}^3 \text{ mol}^{-1} \text{ s}^{-1}$) and oxygen ($k = 3 \times 10^9 \text{ dm}^3 \text{ mol}^{-1} \text{ s}^{-1}$) for O^- formed in the reaction of the hydrated electrons with N_2O provided the oxygen concentration is high enough. By protonation of O_3^- and subsequent dissociation of HO_3 ,⁸ OH radicals form which in turn react with O_3^- and the other radicals and products present. When reaction 10 occurs, ozone is produced and by subsequent reaction with O_2^- the ozonide ion radicals may be regenerated. This effect may be seen from the relatively slow increase of part of the absorbance at 430 nm and from the decay at 260 nm. Under these conditions the decay at 260 nm is due

(11) Hart, E. J.; Brown, W. G.; Bjergbakke, E., submitted for publication in *Radiat. Phys. Chem.*

(12) Brown, W. G.; Hart, E. J. *J. Phys. Chem.* **1978**, *82*, 2539.

(13) Unpublished results.

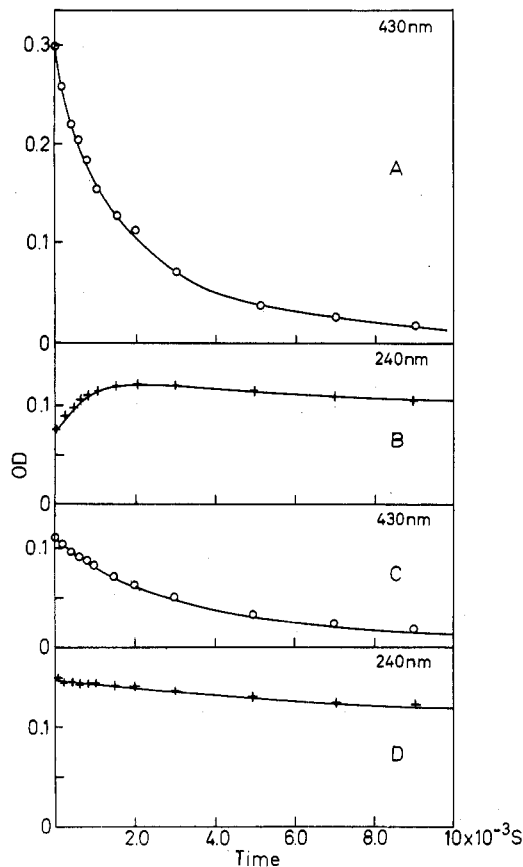
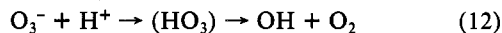


Figure 6. Calculated optical density traces with experimental values for O_3^- decay (430 nm) and O_2^- buildup (240 nm) in 10^{-2} mol dm^{-3} sodium hydroxide (pH 12.0): 1- μs pulse; optical path length, 2.5 cm. A and B: containing 1.25×10^{-3} mol dm^{-3} oxygen and ~ 0.9 mol dm^{-3} nitrous oxide; dose, 10.2 krd. C and D: containing 1.25×10^{-3} mol dm^{-3} oxygen; dose, 8.7 krd. Solid lines: calculated. O, +: experimental values.

not only to reaction 11 but to some extent also to OH radicals from reaction 1 consuming peroxy radicals (reaction 7).

From the fast decay of O_3^- at 430 nm an estimate of the rate constant for the reaction



of $k_{12} = (9 \pm 1) \times 10^{10}$ dm^3 mol^{-1} s^{-1} can be made. This rate

constant agrees with a rate constant derived from experiments with irradiated ozone solutions at pH 3.7.¹⁴ From the experimental half-life of 40 ns for O_3^- , $k(O_3^- + H^+) = 8.5 \times 10^{10}$ dm^3 mol^{-1} s^{-1} . If $k(O_3^- + H^+) = 9 \times 10^{10}$ dm^3 mol^{-1} s^{-1} is used, together with our proposed mechanism in the computer calculations, the absorptions and kinetics at pH 9.5–10.5 may be satisfactorily reproduced. See Figure 5.

Mechanism of O_3^- Decay. In the pH range 10–13 with 4 MPa of N_2O and 0.1 MPa of O_2 , and a 1- μs pulse of approximately 10 krd, the decay kinetics of O_3^- is similar to the decay kinetics at high pHs¹ although faster. This decay is followed by a simultaneous buildup of absorbance in the UV, although the buildup becomes weaker as the pH is lowered. Below pH ~ 11 , no buildup is observed. The UV spectrum remaining after the decay of O_3^- is that of O_2^- , identical with that published in our previous paper. However, the yield of O_2^- is lower. The consumption of O_2^- during the last part of the ozonide ion radical decay increases with decreasing pH due to reaction 7.

In an oxygenated solution under the same pulse conditions there is a slight but continuous decay of O_2^- , as O_3^- decays, again attributed to reaction 7.

A complete reaction scheme for the water radiolysis was used for the computer simulations. This mechanism consists of 49 chemical equations including reactions 1–8 and 10–12. All reactions are well established with known rate constants⁶ except for reactions 6, 10, and 12. The rate constants for these reactions are derived from the present experiments with high-intensity pulses. Excellent agreement between calculated and experimental values of absorbance changes is obtained with atmospheric pressure of O_2 with high-pressure N_2O , and without N_2O over the pH range 10–13. An example of the agreement at pH 12 is shown in Figure 6. The G values for the primary radicals used in the computations are given in Table II. A recalculation of our results at pH 13–13.8 (ref 1) with reactions 6, 10, and 12 included in the mechanism does not alter the satisfactory agreement between experimental and calculated values. This result supports our previous assumption that OH radical reactions do not play an important role at these high pHs.

Acknowledgment. We thank H. Corfitzen and T. Johansen for technical assistance during the work.

Registry No. O_3 , 10028-15-6; O_3^- , 12596-80-4; $\cdot OH$, 3352-57-6; O_2^- , 11062-77-4.

(14) Jonah, C.; Hart, E. J., unpublished results.